



## Enhancement of the steady-state magnetization in TROSY experiments

Roland Riek\*

Institut für Molekularbiologie und Biophysik Eidgenössische Technische Hochschule Hönggerberg CH-8093  
Zürich, Switzerland

E-mail: rr@mol.biol.ethz.ch

Received 10 May 2001; Accepted 16 July 2001

**Key words:** NMR, relaxation delay, steady-state magnetization, transverse relaxation-optimized spectroscopy, TROSY

### Abstract

Under the condition that the longitudinal relaxation time of spin  $I$  is shorter than the longitudinal relaxation time of spin  $S$  the steady-state magnetization in  $[S, I]$ -TROSY-type experiments can be enhanced by intermediate storage of a part of the steady-state magnetization of spin  $I$  on spin  $S$  with a pulse sequence element during the relaxation delay. It is demonstrated with samples ranging in size from the 1 kDa cyclosporin to the 110 kDa  $^{15}\text{N}$ ,  $^2\text{H}$ -labeled dihydroneopterin Aldolase that intermediate storage of steady-state magnetization in a  $[^{15}\text{N}, ^1\text{H}]$ -TROSY experiment yields a signal gain of 10–25%. The method proposed here for intermediate storage of steady-state magnetization can be implemented in any  $[^{15}\text{N}, ^1\text{H}]$ -TROSY-type experiments.

### Introduction

The equilibrium magnetization, which is in a multiscan experiment replaced by the steady-state magnetization, is a prerequisite of NMR experiments (Abragam, 1961). The size of the equilibrium magnetization is directly correlated with the sensitivity of an experiment. Thus, any enhancement of the steady-state magnetization increases the sensitivity of NMR experiments. Methods used so far to enhance equilibrium magnetization include increases in the static magnetic fields, transfer of the high spin polarization of unpaired electrons to coupled nuclear spins through microwave irradiation in solid state NMR (Hall et al., 1993) or use of the polarization transfer from optically polarized xenon to surface and solution spins (Navon et al., 1996). The pulse sequence element INEPT (Morris and Freeman, 1979) enhances insensitive nuclei by polarization transfer from sensitive nuclei, whereas the implementation of the Ernst angle yields signal enhancement by accounting for the finite rate of recovery of equilibrium magnetization (Ernst

et al., 1987; Ross et al., 1998). In TROSY-type experiments (Pervushin et al., 1997; Riek et al., 2000) a signal enhancement has been achieved by merging two different steady-state magnetizations (Pervushin et al., 1998a, b; Brutscher et al., 1998; Riek et al., 2001). Now, we demonstrate that the steady-state magnetization in  $[S, I]$ -TROSY-type experiments can be enhanced by intermediate storage of a part of the steady-state magnetization of spin  $I$  on spin  $S$  with a pulse sequence element during the relaxation delay. We name this technique ISIS standing for *I*ncreased *S*teady state magnetization by *I*ntermediate *S*torage.

### Theory

We consider a system of two scalar coupled spins  $I/2$ ,  $I$  and  $S$  with a scalar coupling constant  $J_{IS}$  located in a macromolecule in solution. We define  $T_1(I)$  as the longitudinal relaxation of spin  $I$  and  $T_1(S)$  as the longitudinal relaxation of spin  $S$ . The gyromagnetic ratio of spin  $I$  is  $\gamma_I$  and for spin  $S$   $\gamma_S$ , with  $\gamma_I > \gamma_S$ . We make the assumption  $T_1(I) < T_1(S)$ .

A conventional  $[S, I]$ -TROSY-type experiment (Pervushin et al., 1997) can be summarized as follows:

\*Present address: Structural Biology Laboratory, The Salk Institute, La Jolla, CA 92037, U.S.A. E-mail: riek@sbl.salk.edu

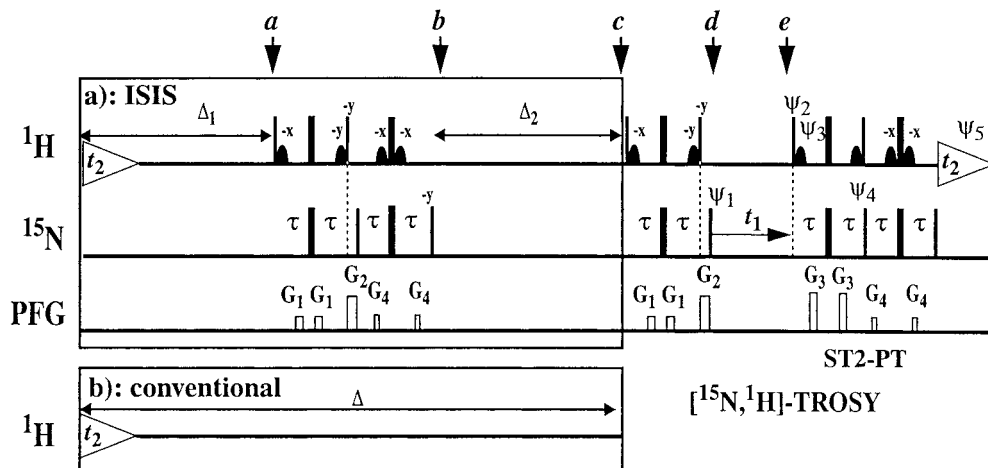


Figure 1. (a) ISIS- $^{15}\text{N}$ , $^1\text{H}$ -TROSY experiment. (b) Conventional  $^{15}\text{N}$ , $^1\text{H}$ -TROSY experiment (Pervushin et al., 1998b). For the conventional  $^{15}\text{N}$ , $^1\text{H}$ -TROSY experiment only the part which differs from (a) is shown and enclosed by a rectangle. The narrow and wide black bars indicate non-selective  $90^\circ$  and  $180^\circ$  pulses, respectively. The radio-frequency pulses on  $^1\text{H}$  and  $^{15}\text{N}$  were applied at 4.8 and 119 ppm, respectively. On the line marked  $^1\text{H}$ , the rounded pulses indicate selective  $90^\circ$  pulses with a duration of 1.1 ms and a Gaussian shape truncated at 5%, which are applied on the water resonance. The line marked PFG indicates sine-shaped pulsed magnetic field gradients applied along the z-axis with the following durations and amplitudes:  $G_1$ , 200  $\mu\text{s}$  and 25 G/cm,  $G_2$ , 200  $\mu\text{s}$  and 20 G/cm,  $G_3$ , 200  $\mu\text{s}$  and 23 G/cm,  $G_4$ , 200  $\mu\text{s}$  and 21 G/cm. The delay  $\tau$  is optimized for the different samples to values ranging from 1.5 ms to 2.7 ms (Riek et al., 1999),  $\Delta_1 + \Delta_2 = \Delta$  is set according to Equation 3 and the ratio  $\Delta_1/\Delta_2$  is between 1:1 and 1:2. The phase cycle is  $\Psi_1 = \{y, -y, x, -x\}$ ,  $\Psi_2 = \{-y\}$ ,  $\Psi_3 = -\Psi_2$ ,  $\Psi_4 = \{-y\}$ ,  $\Psi_5 = \{y, -y, -x, x\}$ . Unless otherwise indicated radio-frequency pulses have a phase  $x$ . In the  $t_1$  ( $^{15}\text{N}$ ) dimension a phase-sensitive spectrum is obtained by recording a second FID for each increment of  $t_1$ , with  $\Psi_1 = \{y, -y, -x, x\}$ ,  $\Psi_2 = \{y\}$ ,  $\Psi_3 = -\Psi_2$ ,  $\Psi_4 = \{y\}$ , and the data is processed as described by Kay et al. (1992). The water magnetization is maintained along the  $+z$  axis throughout the experiment by the use of water flip-back pulses (Grzesiek and Bax, 1993). Residual transverse water magnetization is suppressed by a WATERGATE sequence (Piotto et al., 1992) immediately before data acquisition.

The steady-state magnetization of spin  $I$  is transferred to spin  $S$  via a polarization transfer element and merged with the steady-state magnetization of spin  $S$ . After frequency labeling on spin  $S$  and possibly several additional pulse sequence elements magnetization is transferred back to spin  $I$  and detected during the acquisition (Figure 1b). During the relaxation delay  $\Delta$  consisting of the acquisition period and the following interscan delay the magnetization relaxes back towards the equilibrium (Wider, 1998) resulting in a density matrix at time point  $c$  of the pulse sequence (Abragam, 1961):

$$\sigma(c) = \gamma_I \left(1 - \exp\left(-\frac{\Delta}{T_1(I)}\right)\right) I_z + \gamma_S \left(1 - \exp\left(-\frac{\Delta}{T_1(S)}\right)\right) S_z. \quad (1)$$

During the first polarization transfer element of a  $[S, I]$ -TROSY-type experiment with the phase  $\Psi_1 = x$ , the steady-state magnetization of spin  $I$  (first term in Equation 1) is transferred to  $I_z S_y$  and combined at time point  $d$  in Figure 1b with the steady-state magnetization of spin  $S$  (second term in Equation 1):

$$\sigma(d) = u\gamma_I \left(1 - \exp\left(-\frac{\Delta}{T_1(I)}\right)\right) I_z S_y + \gamma_S \left(1 - \exp\left(-\frac{\Delta}{T_1(S)}\right)\right) S_y, \quad (2)$$

where  $u$  ( $0 < u < 1$ ) indicates the magnetization loss during the polarization transfer element and the longitudinal relaxation of spin  $S$  during the short time period  $\tau$  ( $\tau \ll \Delta$ ) is neglected. As indicated by Equations 1 and 2 the sensitivity of an experiment strongly depends on the relaxation delay  $\Delta$ . The optimal relaxation delay  $\Delta$  for maximal sensitivity relative to the total measuring time of the experiment is given by Equation 3 (Ernst et al., 1987, p. 155)

$$\Delta = 1.269T_1(I), \quad (3)$$

when we neglect the steady-state magnetization of spin  $S$ , since its contribution to the overall steady-state magnetization is small under the assumptions  $\gamma_I > \gamma_S$ ,  $T_1(I) < T_1(S)$  and  $u \approx 1$ .

We demonstrate in the following, that the steady-state magnetization can be enhanced by intermediate storage of the  $I$  steady-state magnetization on spin  $S$ . We term this technique ISIS. The intermediate storage takes place during the relaxation delay  $\Delta$  where

$\Delta$  is divided into two sections  $\Delta_1$  and  $\Delta_2$  (see Figure 1a). After the time period  $\Delta_1$  at the time point  $a$ , magnetization on spin  $I$

$$\sigma(a) = \gamma_I \left( 1 - \exp \left( -\frac{\Delta_1}{T_1(I)} \right) \right) I_z \quad (4)$$

is transferred to  $S_z$  via a pulse sequence element (such as that shown between time point  $a$  and  $b$  of Figure 1a) to:

$$\sigma(b) = uv\gamma_I \left( 1 - \exp \left( -\frac{\Delta_1}{T_1(I)} \right) \right) S_z, \quad (5)$$

where  $u$  takes account of the magnetization loss during the first INEPT (Morris and Freeman, 1979) and  $v$  ( $0 < v < 1$ ) represents the magnetization loss during the refocusing element, which converts  $I_z S_y$  to  $S_z$ . During the period  $\Delta_2$ , the magnetizations of spin  $I$  and spin  $S$  relax once more towards equilibrium. Thus, the total steady-state magnetization at time point  $c$  is given by Equation 6

$$\begin{aligned} \sigma(c) = & \gamma_I \left( 1 - \exp \left( -\frac{\Delta_2}{T_1(I)} \right) \right) I_z \\ & + \gamma_S \left( 1 - \exp \left( -\frac{\Delta_2}{T_1(S)} \right) \right) S_z \\ & + uv\gamma_I \left( 1 - \exp \left( -\frac{\Delta_1}{T_1(I)} \right) \right) \\ & \exp \left( -\frac{\Delta_2}{T_1(S)} \right) S_z. \end{aligned} \quad (6)$$

After the following polarization transfer with  $\Psi_1 = x$  between time points  $c$  and  $d$  of Figure 1a the steady-state magnetizations of spin  $S$  and  $I$  are merged finally to obtain

$$\begin{aligned} \sigma(d) = & uv\gamma_I \left( 1 - \exp \left( -\frac{\Delta_2}{T_1(I)} \right) \right) I_z S_y \\ & + \gamma_S \left( 1 - \exp \left( -\frac{\Delta_2}{T_1(S)} \right) \right) S_y \\ & + uv\gamma_I \left( 1 - \exp \left( -\frac{\Delta_1}{T_1(I)} \right) \right) \\ & \exp \left( -\frac{\Delta_2}{T_1(S)} \right) S_y. \end{aligned} \quad (7)$$

The ISIS- $^{15}\text{N}, ^1\text{H}$ -TROSY experiment (Equation 7 and Figure 1a) is more sensitive than the conventional experiment (Equation 2 and Figure 1b) when the following relation is fulfilled

$$v \exp \left( -\frac{\Delta_2}{T_1(S)} \right) > \exp \left( -\frac{\Delta_2}{T_1(I)} \right). \quad (8)$$

The small contribution of the  $S$  steady-state magnetization was neglected in Equation 8 and it was assumed that  $\Delta_1 + \Delta_2 = \Delta$ , where  $4\tau \ll \Delta_1 + \Delta_2$ .

Thus, if  $T_1(I) < T_1(S)$  and  $v \approx 1$  intermediate storage of steady-state magnetization of spin  $I$  on spin  $S$  (ISIS) enhances the overall usable steady-state magnetization.

## Experimental

$^{15}\text{N}$ -labeled Cyclosporin A, a cyclic peptide with 11 residues, was measured in chloroform at 20 °C on a BRUKER DRX 600 MHz spectrometer equipped with four radio-frequency channels and shielded pulsed field gradients along the  $z$ -direction. The peptide concentration was about 1 mM.

The NMR experiments with 7,8-dihydroneopterin Aldolase from *Staphylococcus aureus* (DHNA) were recorded on a Bruker DRX-750 spectrometer equipped with four radio-frequency channels and shielded pulsed field gradients along the  $z$ -direction. This protein is a homo-octamer with subunits of 121 amino acid residues and a total molecular weight of 110 kDa. The DHNA sample used is uniformly isotope-labeled with  $^{15}\text{N}$  and to the extent of 75% with  $^2\text{H}$ . Measurements with DHNA were conducted at 20 °C in  $\text{H}_2\text{O}$  at a protein concentration of 0.4 mM (Salzmann et al., 2000).

$^{15}\text{N}, ^2\text{H}$ -labeled Outer membrane protein A (OmpA) with a molecular weight 16 kDa was measured at 30 °C on a BRUKER DRX 600 MHz spectrometer in a aqueous solution of lipid micelles (3% Dihexanoyl-phosphatidylcholine). The protein concentration was about 1 mM (Fernandez et al., 2001).

## Results

Based on theoretical calculations, signal enhancement for TROSY-type experiments can be obtained using ISIS when  $T_1(I) < T_1(S)$ . These conditions are met for  $^{15}\text{N}, ^1\text{H}$ -backbone moieties of proteins where  $T_1(^1\text{H}) < T_1(^{15}\text{N})$  (unpublished results). Thus, ISIS was implemented in a  $^{15}\text{N}, ^1\text{H}$ -TROSY experiment (Figure 1a). After the relaxation delay  $\Delta_1$  the proposed pulse sequence element for ISIS transfers magnetization *via* a refocusing INEPT (Morris and Freeman, 1979) from  $I_z \rightarrow I_y \rightarrow 2I_x S_z \rightarrow 2I_z S_z \rightarrow 2I_z S_y \rightarrow S_x \rightarrow S_z$ . The refocusing INEPT is followed by the relaxation delay  $\Delta_2$ . The ISIS- $^{15}\text{N}, ^1\text{H}$ -TROSY (Figure 1a) was compared with the conventional  $^{15}\text{N}, ^1\text{H}$ -TROSY type experiment for three molecules:  $^{15}\text{N}$ -labeled Cyclosporin A measured

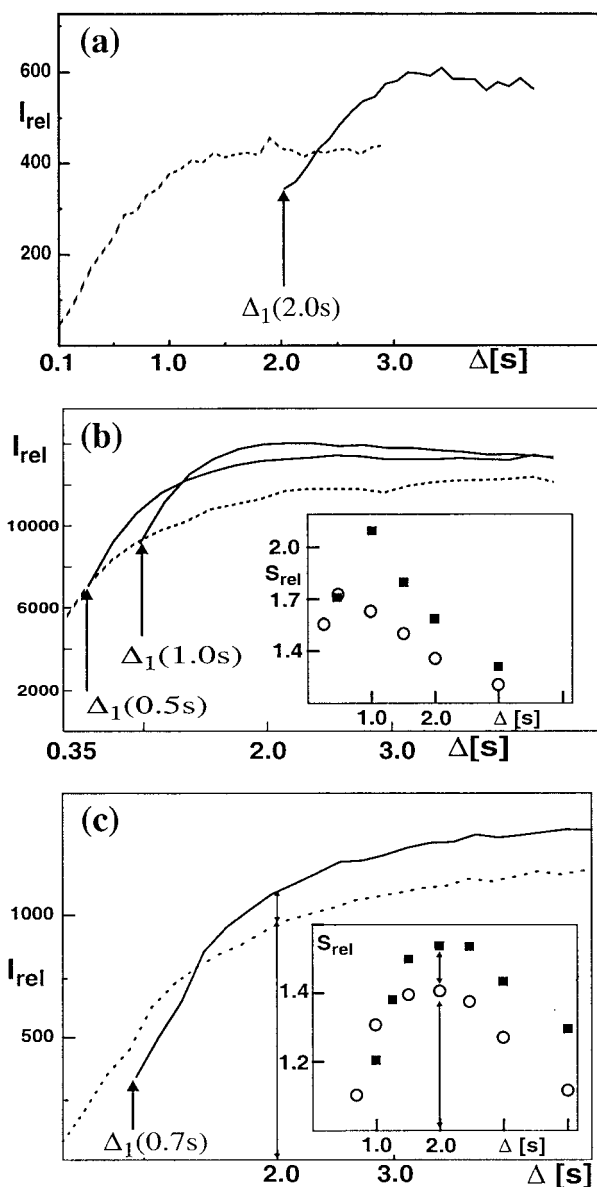


Figure 2. Build-up curves of the steady-state magnetization versus relaxation delay  $\Delta$  for three molecules (a)  $^{15}\text{N},^2\text{H}$ -labeled OmpA, (b)  $^{15}\text{N}$ -labeled Cyclosporin A, and (c)  $^{15}\text{N},^2\text{H}$ -labeled DHNA. In each case the conventional build-up curve of the  $^{15}\text{N},^1\text{H}$ -TROSY of Figure 1b (dotted line) is compared to build-up curves of the ISIS- $^{15}\text{N},^1\text{H}$ -TROSY of Figure 1a (straight line). For the ISIS- $^{15}\text{N},^1\text{H}$ -TROSY experiment the relaxation delay  $\Delta$  is composed of the two delays  $\Delta_1$  and  $\Delta_2$ . For each ISIS build-up curve,  $\Delta_1$  is held fixed whereas  $\Delta_2$  is incremented with the starting value 0. In (a)  $\Delta_1 = 2.0$  s as indicated. In (b) two ISIS build-up curves are measured with  $\Delta_1 = 0.5$  s and  $\Delta_1 = 1.0$  s, respectively, as indicated by the arrows. In (c)  $\Delta_1 = 0.7$  s and the optimal relaxation delay (Ernst et al., 1987)  $\Delta = 2.0$  s is indicated by an arrow. The two insets to (b) and (c) show the sensitivity  $S_{\text{rel}}$  of the ISIS- $^{15}\text{N},^1\text{H}$ -TROSY (black squares) and the  $^{15}\text{N},^1\text{H}$ -TROSY (circles) in function of the relaxation delay  $\Delta$ .  $S_{\text{rel}}$  is defined as relative signal to noise per measuring time. The sensitivity plots of the ISIS- $^{15}\text{N},^1\text{H}$ -TROSY are measured with a fixed delay  $\Delta_1 = 0.5$  s in (b) and  $\Delta_1 = 0.7$  s in (c), respectively. All build-up curves were measured based on one dimensional versions of the pulse sequences of Figure 1. For the build-up curve in the conventional experiment the relaxation delay  $\Delta$  is incremented in steps of 0.2 s. For the ISIS build-up curve,  $\Delta_2$  is incremented in steps of 0.2 s with a fixed  $\Delta_1$  as indicated. For each increment 64 scans were measured. The signal intensities,  $I_{\text{rel}}$ , of the peaks were measured for the build-up curves.

in chloroform,  $^{15}\text{N}$ , $^2\text{H}$ -labeled 7,8-dihydroneopterin Aldolase (DHNA) measured in water and  $^{15}\text{N}$ , $^2\text{H}$ -labeled Outer membrane protein A (OmpA) measured in a water/micelle mixture. These three molecules span a range of sizes from 1 to 110 kDa and correspondingly a range of  $T_1$  and  $T_2$  relaxation times for  $^1\text{H}$  and  $^{15}\text{N}$ , respectively. In Figure 2a the dotted line represents the build-up curve of the steady-state magnetization in a  $^{15}\text{N}$ , $^1\text{H}$ -TROSY (Figure 1b) *versus* the relaxation delay  $\Delta$  measured with the  $^{15}\text{N}$ , $^2\text{H}$ -labeled OmpA. After two seconds the steady-state magnetization has essentially reached the equilibrium value. In addition, a build-up curve of the ISIS- $^{15}\text{N}$ , $^1\text{H}$ -TROSY is shown which was obtained using the pulse sequence of Figure 1a with an arbitrary fixed delay  $\Delta_1 = 2.0$  s and increasing delays  $\Delta_2$ . Thus, the steady-state magnetization recovered on  $^1\text{H}$  after two seconds of relaxation is stored on  $^{15}\text{N}$ . In the initial points of the ISIS build-up curve ( $\Delta = \Delta_1 = 2.0$  s up to  $\Delta = \Delta_1 + \Delta_2 = 2.0$  s + 0.4 s) ISIS- $^{15}\text{N}$ , $^1\text{H}$ -TROSY is less sensitive than the conventional  $^{15}\text{N}$ , $^1\text{H}$ -TROSY due to the loss of  $^{15}\text{N}$  steady-state magnetization and due to the transverse relaxation of  $^{15}\text{N}$  which is active during the additional INEPT and which is taken into consideration in equations 5–8 by the factor  $v$ . For longer delays  $\Delta_2$  ( $\Delta_2 > 0.5$ ,  $\Delta_1 = 2.0$  s) sufficient recovery of the proton steady-state magnetization during the delay  $\Delta_2$  combined with the intermediately storage of  $^1\text{H}$  steady-state magnetization on  $^{15}\text{N}$  results in a superior signal intensity (Figure 2a). After  $\Delta = 3.0$  s signal enhancements of up to 50% was achieved. This example shows nicely the principle of ISIS: Steady-state magnetization of  $^1\text{H}$  at time point  $\Delta_1 = 2$  s is stored on  $^{15}\text{N}$  and during the delay  $\Delta_2$   $^1\text{H}$  steady-state magnetization is recovered. However, from an experimental point of view the keen interest is the signal enhancement per measuring time, which is unfortunately less pronounced and which will be discussed in the following.

The ISIS- $^{15}\text{N}$ , $^1\text{H}$ -TROSY experiments of Cyclosporin A with the delays  $\Delta_1 = 0.5$  s or 1.0 s and  $\Delta_2 > 0$  s are superior to the conventional experiment with a corresponding delay  $\Delta$  (Figure 2b). Since the  $^{15}\text{N}$  transverse relaxation time  $T_2(^{15}\text{N})$  is small in the case of small molecules there is almost no signal lost during the additional pulse sequence element ( $v \approx 1$ ) and the loss of the  $^{15}\text{N}$  steady-state magnetization diminishes only minor the signal intensities due to a long effective  $T_1(^{15}\text{N})$  of 2.5 s. The superiority of the ISIS technique is further shown by the plots of the sensitiv-

ity  $S_{\text{rel}}$  of the TROSY-experiments in function of the delay  $\Delta$  (inset to Figure 2b). The sensitivity  $S_{\text{rel}}$  is defined as signal intensity relative to the total measuring time. As can be inferred from the inset of Figure 2b, the ISIS- $^{15}\text{N}$ , $^1\text{H}$ -TROSY experiment with the optimal delays  $\Delta_1 = 0.5$  s and  $\Delta_2 = 0.5$  is 20% more sensitive than the conventional  $^{15}\text{N}$ , $^1\text{H}$ -TROSY experiment with an optimal relaxation delay  $\Delta = 0.5$  s (inset to Figure 2c).

Finally, Figure 2c shows for 110 kDa DHNA that the ISIS- $^{15}\text{N}$ , $^1\text{H}$ -TROSY obtains results superior to the conventional experiment as can be inferred from comparison of the two build-up curves and the two sensitivity plots.

For optimal sensitivity in conventional experiments the relaxation delay  $\Delta$  should be adjusted using either equation 3 or an experimental build-up curve or a sensitivity curve as presented in Figure 2. According to the inset of Figure 2c the optimal sensitivity for DHNA is obtained with  $\Delta = 2$  s. Indeed, a 2D  $^{15}\text{N}$ , $^1\text{H}$ -TROSY (Figure 1b) with a  $\Delta = 2$  s was more sensitive than the 2D  $^{15}\text{N}$ , $^1\text{H}$ -TROSY experiment with  $\Delta = 1$  s measured in the same total time using twice the number of scans. The measured sensitivity difference of about 5% (data not shown) compares well with the calculated sensitivity difference of 5.5% using Equation 3. Also the combination of a 2D  $^{15}\text{N}$ , $^1\text{H}$ -TROSY with  $\Delta = 1.3$  s with an experiment with  $\Delta = 0.7$  s was about 10% less sensitive than the TROSY with  $\Delta = 2$  s, as expected (data not shown).

In the case of the ISIS- $^{15}\text{N}$ , $^1\text{H}$ -TROSY (Figure 1 and Equation 7) the sensitivity of the proposed experiment depends on  $T_1(^1\text{H})$ ,  $T_1(^{15}\text{N})$  and  $T_2(^{15}\text{N})$  and the delays  $\Delta_1$  and  $\Delta_2$ . If relaxation data are not available, optimal sensitivity can be obtained by experimental adjustments of the delays  $\Delta_1$  and  $\Delta_2$ . For this purpose we propose the measurement of two to three different build-up curves as shown in Figure 2. Otherwise, we find that the optimal ratio  $\Delta_1/\Delta_2$  with an optimal relaxation delay  $\Delta$  is between 1:1 and 1:2 and that the curve corresponding to the signal enhancement *versus*  $\Delta_1/\Delta_2$  has a rather broad maximum. For DHNA optimal sensitivity for the intermediate storage of steady-state magnetization is obtained with  $\Delta_1 = 0.7$  s and  $\Delta_2 = 1.3$  s (see Figure 2c). Using these delays in a 2D ISIS- $^{15}\text{N}$ , $^1\text{H}$ -TROSY experiment signal enhancements of 10–25% are observed in comparison to the corresponding signals using the conventional experimental set-up measured in the same total time with an optimal relaxation delay  $\Delta = 2$  s (Figure 3).

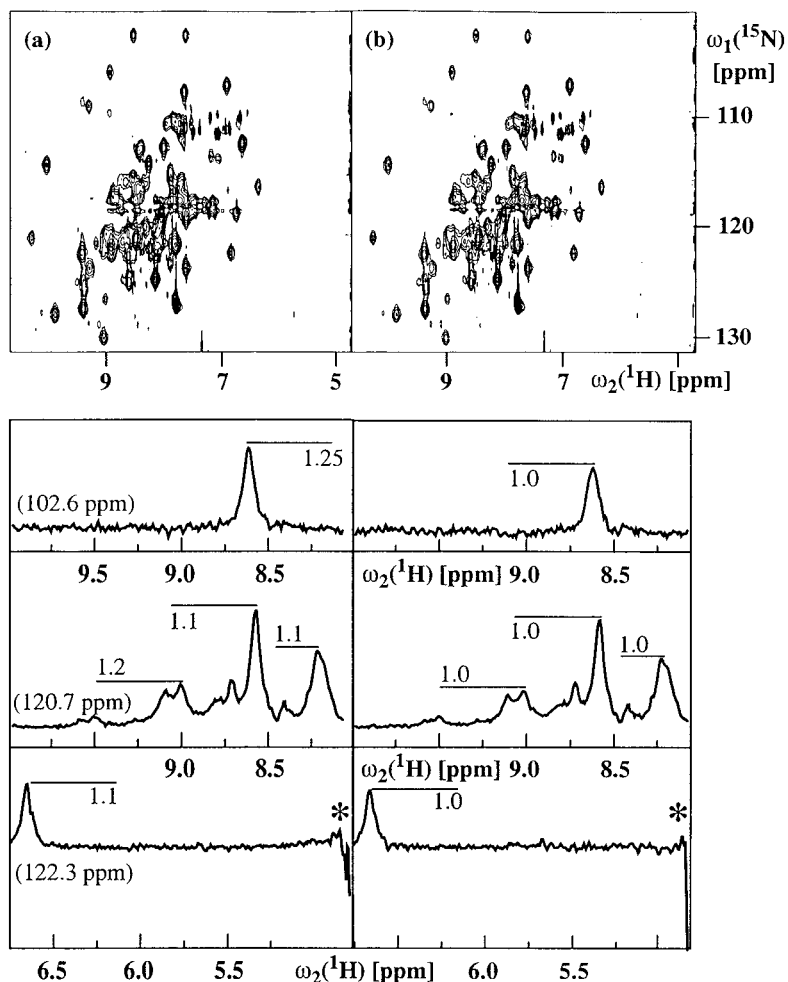


Figure 3. 2D  $^{15}\text{N}, ^1\text{H}$ -TROSY spectra including cross-sections of  $^{15}\text{N}, ^2\text{H}$ -labeled DHNA. (a) ISIS- $^{15}\text{N}, ^1\text{H}$ -TROSY spectrum. (b)  $^{15}\text{N}, ^1\text{H}$ -TROSY spectrum. For optimal sensitivity the parameters are set as follows:  $\tau = 1.75$  ms (see Riek et al., 1999),  $\Delta = 2.0$  s,  $\Delta_1 = 0.7$  s, and  $\Delta_2 = 1.3$  s. The measurement time for each experiment was 1 hour, and the acquired data size was  $60 \times 1024$  complex points and the processed spectra contained  $256 \times 2048$  points after zero filling. The time domains were  $t_{1,\text{max}} = 32$  ms,  $t_{2,\text{max}} = 100$  ms for both experiments. The relative peak amplitudes are indicated with a horizontal line and a number. '\*' designates the water resonance.

The average signal enhancement of 1.12 was observed with a standard deviation of 0.05.

## Discussion

Steady-state magnetization can be enhanced using a pulse sequence element during the relaxation delay which stores part of the steady-state magnetization of spin  $I$  on spin  $S$  by taking the advantage of the difference in longitudinal relaxation times between  $I$  and  $S$  spins. This pulse sequence element can be implemented in any  $^{15}\text{N}, ^1\text{H}$ -TROSY-type 2D, 3D, or 4D experiment (Pervushin et al., 1997, 1998b; Loria et

al., 1999a, b; Yang and Kay, 1999; Salzmann et al., 1998, 2000) and yields up to 25% signal enhancement (Figure 3). Theoretically, the ISIS technique can be furthermore optimized with additional elements. However, the enhancement would follow a geometric progression with an asymptotic limit, since magnetization is lost during each pulse sequence element.

Another interesting observation is the similarity between the proposed pulse sequence element within ISIS and the single-transition to single-transition polarization transfer element (ST2-PT element; Pervushin et al., 1998b) of the  $^{15}\text{N}, ^1\text{H}$ -TROSY experiment (Figure 1a). Indeed, the ST2-PT element transfers  $^{15}\text{N}$  single-transition coherences to  $^1\text{H}$  single-

transition coherences and simultaneously longitudinal  $^1\text{H}$  magnetization to longitudinal  $^{15}\text{N}$  magnetization. Thus, in a conventional [ $^{15}\text{N}$ ,  $^1\text{H}$ ]-TROSY experiment, the steady-state magnetization of  $^1\text{H}$  at the time point  $e$  (Figure 1b) is stored on  $^{15}\text{N}$  and used in the next scan of the experiment. Usually, its contribution to the overall steady-state magnetization is small due to a short  $t_1$  and a long interscan delay  $\Delta$  (replace  $\Delta_2$  in Equation 7 with  $\Delta$  and  $\Delta_1$  with  $t_1$ , respectively). However, in the reference experiment of the  $^{15}\text{N}\{^1\text{H}\}$ -NOE- $^{15}\text{N}$ ,  $^1\text{H}$ -TROSY experiment (Zhu et al., 2000), the steady-state magnetization of  $^1\text{H}$  stored on  $^{15}\text{N}$  due to the ST2-PT element overwhelms the desired  $^{15}\text{N}$  steady-state magnetization (data not shown), because of the small size of the desired  $^{15}\text{N}$  steady-state magnetization (second term of equation 1 with a  $\gamma_S \approx \gamma_I/10$ ) relative to the steady-state magnetization of  $^1\text{H}$ , which relaxes during the interscan delay  $\Delta$  and is transferred to  $^{15}\text{N}$  with the ST2-PT element (last term of Equation 7 with  $\Delta_1 = \Delta_2 = \Delta$ ). Therefore, this unwanted steady-state magnetization from  $^1\text{H}$  must be suppressed as for example was proposed by Zhu et al. (2000).

In conclusion, it is intriguing that with a pulse sequence element during the relaxation delay the steady-state magnetization can be enhanced. The ISIS technique yields reasonable signal enhancement in [ $^{15}\text{N}$ ,  $^1\text{H}$ ]-TROSY experiments over a wide range of molecular sizes between 1 kDa and 110 kDa and can be implemented easily in other [ $^{15}\text{N}$ ,  $^1\text{H}$ ]-TROSY-type experiments.

### Acknowledgements

We thank Prof Dr Kurt Wüthrich for generously providing the protein samples and access to NMR instrumentation. We thank Dr Fred Damberger for careful reading of the manuscript and helpful discussions. Financial support was obtained from the Schweizerischer Nationalfonds (Project 31.49047.96).

### References

- Abragam, A. (1961) *The Principles of Nuclear Magnetism*, Clarendon, Oxford.
- Brutscher, B., Boisbouvier, J., Pardi, A., Marion, D. and Simorre, J.P. (1998) *J. Am. Chem. Soc.*, **120**, 11845–11851.
- Ernst, R.R., Bodenhausen, G. and Wokaun, A. (1987). *The Principles of Nuclear Magnetic Resonance in One and Two Dimensions*, Clarendon, Oxford.
- Fernandez, C., Adeishvili, K. and Wüthrich, K. (2001) *Proc. Natl. Acad. Sci. USA*, **98**, 2358–2363.
- Grzesiek, S. and Bax, A. (1993) *J. Am. Chem. Soc.*, **115**, 12593–12594.
- Hall, D.A., Maus, D.C., Gerfen, G.J., Inati, S.J., Becerra, L.R., Dahlquist, F.W. and Griffin R.G. (1993) *Science*, **276**, 930–932.
- Kay, L.E., Keifer, P. and Saarinen, T. (1992) *J. Am. Chem. Soc.*, **114**, 10663–10664.
- Loria, J.P., Rance, M. and Palmer, A.G. (1999a) *J. Biomol. NMR.*, **141**, 151–155.
- Loria, J.P., Rance, M. and Palmer, A.G. (1999b) *J. Magn. Reson.*, **141**, 180–184.
- Morris, G.A. and Freeman, R. (1979) *J. Am. Chem. Soc.*, **101**, 760–762.
- Navon, G., Song, Y.Q., Room, T., Appelt, S., Taylor, R.E. and Pines A. (1996) *Science*, **271**, 1848–1851.
- Pervushin, K., Riek, R., Wider, G. and Wüthrich, K. (1997) *Proc. Natl. Acad. Sci. USA*, **94**, 12366–12371.
- Pervushin, K., Riek, R., Wider, G. and Wüthrich, K. (1998a) *J. Am. Chem. Soc.*, **120**, 6394–6400.
- Pervushin, K., Wider, G. and Wüthrich, K. (1998b) *J. Biomol. NMR*, **12**, 345–348.
- Pervushin, K., Wider, G., Riek, R. and Wüthrich, K. (1999) *Proc. Natl. Acad. Sci. USA*, **96**, 9607–9612.
- Piotto, M., Saudek, V. and Sklenar, V.J. (1992) *J. Biomol. NMR*, **2**, 661–665.
- Riek, R., Pervushin, K., Fernandez, C., Kainosho, M. and Wüthrich, K. (2001) *J. Am. Chem. Soc.*, **123**, 658–664.
- Riek, R., Pervushin, K. and Wüthrich, K. (2000) *Trends Biochem. Sci.*, **25**, 462–468.
- Riek, R., Wider, G., Pervushin, K. and Wüthrich, K. (1999) *Proc. Natl. Acad. Sci. USA*, **96**, 4918–4923.
- Ross, A., Salzmann, M. and Senn, H. (1998) *J. Biomol. NMR*, **10**, 389–396.
- Salzmann, M., Pervushin, K., Wider, G., Senn, H. and Wüthrich, K. (1998) *Proc. Natl. Acad. Sci. USA*, **95**, 13585–13590.
- Salzmann, M., Pervushin, K., Wider, G., Senn, H. and Wüthrich, K. (2000) *J. Am. Chem. Soc.*, **122**, 7543–7548.
- Wider, G. (1998) *Prog. NMR Spectr.*, **32**, 193–275.
- Yang, D.W. and Kay, L.E. (1999) *J. Am. Chem. Soc.*, **121**, 2571–2575.
- Zhu, G., Xia, Y.L., Nicholson, L.K. and Sze, K.H. (2000) *J. Magn. Reson.*, **143**, 423–426.